Viscoelastic Contact Resonance Force Microscopy of Polymers in Liquid

Allison B. Churnside†, Ryan C. Tung, Jason P. Killgore

National Institue of Standards and Technology, Boulder, CO
† Corresponding author: allison.churnside@nist.gov

ABSTRACT

Contact resonance force microscopy (CR-FM) is an atomic force microscope (AFM) based technique for quantitatively measuring mechanical properties. Measurements in liquid are key to many materials, particularly biological materials. However, liquid CR-FM is complicated by spurious resonances and difficulty in separating mechanical properties of the material from liquid effects on the probe. Spurious resonances can be avoided by using direct cantilever excitation for well-separated resonance peaks in liquid. Liquid effects can be accounted for with a reconstructed hydrodynamic function. We used this reconstruction to correct CR-FM loss tangents (tan(δ)) in water, and compared tan(δ) of polystyrene and polypropylene measured in air and water. Using the hydrodynamic correction, the values in air agreed with those in water. This demonstrates the validity of the technique, and provides a path forward for nanoscale viscoelastic mapping in liquid environments.

Keywords: atomic force microscope, contact resonance, liquid environment, nanomechanics, polymers

1 INTRODUCTION

The viscoelastic properties of soft materials such as polymers and cells are central to their functionality, but their measurement can be challenging. Atomic force microscope (AFM) based techniques can provide viscoelastic information with nanoscale spatial resolution [1]. Much work has been put into quantitatively measuring elastic properties of materials with AFM [2-4]. The viscous damping is also a critical parameter needed to characterize many materials, but it is more difficult to measure accurately [5,6]. Additional complications arise when the measurements must be done in liquid, for instance in biological applications. In this paper we present measurements of viscoelastic loss tangents measured in water that agree with those measured in air. This new measurement capability opens up new avenues for study of the mechanical properties of hydrated samples.

1.1 Contact resonance force microscopy

Contact resonance force microscopy (CR-FM) [7] is a leading technique for quantitatively determining the nanoscale mechanical properties of materials [1,5]. In CR-FM, the resonant properties of an AFM cantilever in contact with a sample are measured (Figure 1), and interpreted as viscoelastic properties of the sample. Specifically, the storage modulus E' can be determined from the frequency shift upon contact, while the loss modulus E'' can be determined from a combination of the frequency shift and the change in mechanical quality factor Q. In CR-FM, the tip is in constant contact with the surface. This is in contrast to force-extension [3], resonant tapping [8], or peak force tapping [9] modes, where the tip is in intermittent contact with the surface. The constant tip-sample contact, combined with on-resonance sensitivity enhancement and operation in a linear tip-sample contact regime, can result in very accurate property measurements. In addition to E' and E'' it is advantageous to compute loss tangent ($\tan(\delta) = E''/E'$) directly, which avoids uncertainty associated with force and contact geometry [10].

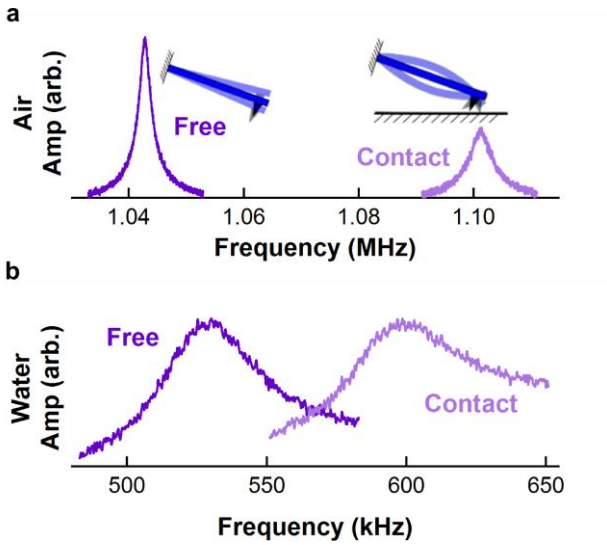

Figure 1. Characteristics of free and contact resonant peaks of AFM cantilevers in contact with a surface, in this case polystyrene. (a) In air, the free resonant peak (*dark purple, left*) has a lower frequency and is distinctly narrower (higher Q) than the resonant peak in contact with the surface (*light purple, right*). (b) In water, the frequency shift from the free resonance (*dark purple, left*) to the resonance in contact (*light purple, right*) is similarly apparent by eye, but the change in peak width is more subtle.

1.2 Operation in a liquid environment

Typically, contact resonance measurements have been made in air, because complications are introduced in a liquid environment. Specifically, it is difficult to excite a cantilever cleanly in a liquid environment [11], and it is difficult to separate the effects of liquid from the effects of the sample under study (Figure 1). However, measurements in a liquid environment are key to characterizing biological materials, tissue scaffolds, medical devices, and many industrial processes, providing motivation for overcoming these difficulties.

In air, cantilever excitation is typically achieved by piezoelectric (acoustic) drive of the cantilever holder. However, driving the cantilever this way in liquid produces a large number of spurious resonances related to coupling between the cantilever holder and fluid droplet, precluding measurement of the cantilever frequency and *Q*. Recent innovations in direct cantilever excitation by use of photothermal [12] and magnetic [13] forcing have enabled measurement of idealized, near-Lorentizan contact resonance peaks in liquid.

Due to surface-coupled fluid effects, the material loss tangent in water is greatly overestimated. Conceptually, this is because background dissipation through the water is measured along with the material dissipation. The dissipation through the water depends on the properties of the fluid, the frequency of the contact resonance, the vibrating shape of the cantilever, and the distance from the cantilever to the surface. Recently our research group developed a model to compensate for the hydrodynamic loading in the contact resonance data [14,15], thus allowing further analysis with existing models. The analysis method relies on reconstruction of the hydrodynamic function based on measurements of the free resonance peaks near the surface. In this way, we are able to correct for the effects of surface-dependent fluid mass loading and damping.

2 METHODS

2.1 Sample preparation

A solution of polystyrene (Goodfellow [16]) dissolved in toluene (Sigma [16]) with a mass fraction of 10% were prepared. Thin (500 nm–1µm) films of polystyrene were prepared by spinning this solution on silicon substrates using a spin coater. Typical spin coater parameters were 3000 rpm for 1 min. These films on silicon were then baked for approximately 1 hour at 110 °C. Polypropylene sheet (Goodfellow) was flattened by heating it to 190 °C sandwiched between two silicon wafers with weight for approximately 12 minutes. The thin polystyrene films were then cut apart from their substrates and floated on water onto the polypropylene. The samples were finally dried by baking at 80 °C for 2.5 hours.

2.2 Data collection

The cantilever was rectangular with a nominal spring constant of 2.8 N/m (FM, NanoWorld [16]) that did not have a metallic coating. It was driven using photothermal excitation (BlueDrive, Asylum Research [16]) at a nominal laser power drive amplitude of 300 µW in air and 1 mW in water. The drive frequency was swept through the resonant peaks at a rate of 2 kHz/s to 150 kHz/s, depending on the width of the peak under examination. If the frequency is swept too fast artifacts occur. In both air and water, data were acquired far from, near to (100 nm to 200 nm), and in contact with each surface. For the near-surface curves, height above the surface was established by touching the tip to the surface and retracting to the desired height. Contact data were collected at approximately 50 nN for polystyrene and 35 nN for polypropylene. These forces were chosen so that the frequency shift upon contact for all modes would be significant, and similar between the two materials. Because different detector laser positions are more or less sensitive to different resonant modes of the cantilever [17], data for all modes was not acquired at the same time. Data in air were acquired at ambient conditions, approximately 40% humidity. Data in water were acquired in ultrapure (18 MΩ-cm) water. Resonant peaks were fit to a driven damped harmonic oscillator equation to recover values for resonant frequency and *Q*.

2.3 Reconstruction of hydrodynamic function

Reconstruction of the hydrodynamic function is described in detail elsewhere [15]. Briefly, the frequency and mechanical quality factors measured approximately 100 nm above the surface at the resonant frequencies were used to determine the real part $\Gamma_r(\mathrm{Re})$ and imaginary part $\Gamma_i(\mathrm{Re})$ of the hydrodynamic function:

$$\Gamma_r(\mathrm{Re}_{\omega_{wet}}) = \frac{\left(\frac{\omega_n}{\omega_{wet}}\right)^2 - 1}{\chi}, \text{ and} \quad (1)$$

$$\Gamma_i(\mathrm{Re}_{\omega_{wet}}) = \frac{\left(\frac{\omega_n}{\omega_{wet}}\right)^2}{Q_{wet}\chi}, \quad (2)$$

where ω_n are the natural frequencies, ω_{wet} and Q_{wet} are the frequencies and mechanical quality factors measured near the surface in water, and the nondimensional parameter $\chi = \frac{\pi}{4}\frac{\rho_f b^2}{\rho A}$, with ρ and ρ_f the densities of the cantilever and the fluid, respectively, b the width of the cantilever, and A its cross-sectional area. The hydrodynamic functions are calculated as a function of the

unsteady Reynolds number $\mathrm{Re} = \frac{\rho_f \omega b^2}{4\mu_f}$, where ω is the near-surface resonant frequency, and μ_f the shear viscosity of the fluid. The hydrodynamic functions $\Gamma_r(\mathrm{Re}_{\omega_{wet}})$ and $\Gamma_i(\mathrm{Re}_{\omega_{wet}})$ were plotted and fitted to

$$\Gamma_r = a_1 + b_1 \mathrm{Re}^{-1/2}, \text{ and} \tag{3}$$

$$\Gamma_i = a_2 + b_2 \mathrm{Re}^{-1/2} + c_2 \mathrm{Re}^{-1}. \tag{4}$$

As shown in Figure 2, this allows us to interpolate the real and imaginary parts of the hydrodynamic function to a range of unsteady Reynolds number (proportional to contact frequency).

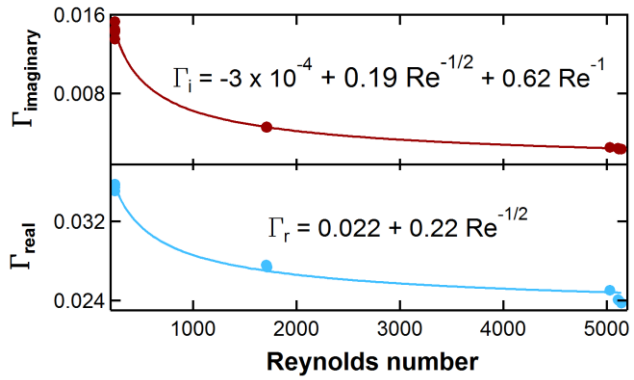

Figure 2. Imaginary (*upper*) and real (*lower*) hydrodynamic functions measured in water and used for the correction in this paper.

2.4 Hydrodynamic correction

Correction of the contact data are also described in detail elsewhere [15]. The corrected contact frequencies were calculated from

$$\omega_{corrected} = \omega_{measured}\left[1 + \chi\Gamma_r(\mathrm{Re}_{\omega_{wet}})\right]^{1/2}. \tag{5}$$

The fluid damping was calculated with

$$Q_{fluid} = \frac{\chi^{-1} + \Gamma_r(\mathrm{Re}_{\omega_{wet}})}{\Gamma_i(\mathrm{Re}_{\omega_{wet}})}, \tag{6}$$

and the damping from contact with the sample is then given by:

$$\frac{1}{Q_{sample}} = \frac{1}{Q_{measured}} - \frac{1}{Q_{fluid}}, \tag{7}$$

where $Q_{measured}$ is the uncorrected quality factor obtained from fitting the resonant peak in contact with the surface.

2.5 Calculation of loss tangent

The loss tangent tan (δ) was computed from the equation

$$\tan\delta = \frac{(\lambda L)^2 \beta}{\alpha} \gamma^2 \frac{\omega_{cont}}{\omega_n}, \tag{8}$$

where α and β are the tip-sample contact stiffness and damping coefficient, respectively, λL is the root of the dispersion relation for the free flexural vibrations of the cantilever, and γ is the ratio of the tip position along the cantilever to its total length [14,18]. To find γ, we used the method of plotting the contact stiffness α for several modes as a function of γ. Assuming that variations in contact stiffness between modes are negligibile, the points where the modes cross give an estimate for γ. Free and contact curves in air were used for this step.

3 RESULTS AND DISCUSSION

3.1 Loss tangent overestimated in water

Without correcting for hydrodynamic effects, the loss tangent for both materials was greatly overestimated in water compared to air (Table 1). Here, in data taken from the second flexural mode of the cantilever, the measured value of tan (δ) for polypropylene in water was a factor of 1.5 higher than in air, while the measured value for polystyrene in water was a factor of 4 higher than in air. The dissipation due to water has a proportionally greater effect on polystyrene. This is as expected because polystyrene has the smaller energy dissipation of the two materials, so the relative effect of the dissipation due to water is greater than for polypropylene.

	Polypropylene	Polystyrene
Air	0.11 ± 0.02	0.014 ± 0.003
Water, uncorrected	0.16 ± 0.02	0.06 ± 0.01
Water, with correction	0.10 ± 0.02	0.02 ± 0.01

Table 1. Loss tangents measured in water are in agreement with those in air after application of the hydrodynamic correction technique for two different polymers. Results are shown as mean value ± standard deviation, with the number of data points *N*=34 for polystyrene in air, *N*=59 for polypropylene in air, *N*=21 for both materials in water.

3.2 Hydrodynamic correction recovers air values

After applying the hydrodynamic correction, the loss tangent for both materials was no longer overestimated. In fact, the corrected values agree to within standard deviations (Table 1). Since the loss tangents of polystyrene and polypropylene are not expected to change upon addition of water, this result provides validation for the hydrodynamic correction technique for these conditions.

4 CONCLUSIONS

CR-FM is a powerful technique for determining the properties of a wide variety of materials, but its use in liquid has been limited because the effect of the sample was difficult to separate from the effect of the liquid. This has limited the materials to which it can be applied. We have shown that by reconstructing the hydrodynamic function of an AFM cantilever near the surface, we can measure loss tangents for polymers in water that agree with those measured in air. This will open up CR-FM to study a wide variety of materials, including biological materials, whose material properties are affected by water or whose measurement is most relevant in water.

Note: this document is an official contribution of the National Institute of Standards and Technology, and not subject to copyright in the United States.

REFERENCES

[1] Hurley, D. C.; Campbell, S. E.; Killgore, J. P.; Cox, L. M.; Ding, Y. "Measurement of Viscoelastic Loss Tangent with Contact Resonance Modes of Atomic Force Microscopy" *Macromolecules* **2013**, *46*, 9396.

[2] Garcia, R.; Proksch, R. "Nanomechanical mapping of soft matter by bimodal force microscopy" *European Polymer Journal* **2013**, *49*, 1897.

[3] Burnham, N. A.; Colton, R. J. "Measuring the nanomechanical properties and surface forces of materials using an atomic force microscope" *Journal of Vacuum Science & Technology A* **1989**, *7*, 2906.

[4] Killgore, J. P.; Hurley, D. C. "Low-force AFM nanomechanics with higher-eigenmode contact resonance spectroscopy" *Nanotechnology* **2012**, *23*, 055702.

[5] Yablon, D. G.; Grabowski, J.; Chakraborty, I. "Measuring the loss tangent of polymer materials with atomic force microscopy based methods" *Measurement Science and Technology* **2014**, *25*, 055402.

[6] Chyasnavichyus, M.; Young, S. L.; Tsukruk, V. V. "Probing of polymer surfaces in the viscoelastic regime" *Langmuir* **2014**, *30*, 10566.

[7] Rabe, U.; Amelio, S.; Kester, E.; Scherer, V.; Hirsekorn, S.; Arnold, W. "Quantitative determination of contact stiffness using atomic force acoustic microscopy" *Ultrasonics* **2000**, *38*, 430.

[8] Tamayo, J.; Garcia, R. "Deformation, contact time, and phase contrast in tapping mode scanning force microscopy" *Langmuir* **1996**, *12*, 4430.

[9] Pittenger, B., Erina, N., and Su, C. In *Nanomechanical Analysis of High Performance Materials*; Tiwari, A., Ed.; Springer: 2014, p 31.

[10] Campbell, S. E.; Ferguson, V. L.; Hurley, D. C. "Nanomechanical mapping of the osteochondral interface with contact resonance force microscopy and nanoindentation" *Acta Biomaterialia* **2012**, *8*, 4389.

[11] Ratcliff, G. C.; Erie, D. A.; Superfine, R. "Photothermal modulation for oscillating mode atomic force microscopy in solution" *Applied Physics Letters* **1998**, *72*, 1911.

[12] Li, Q.; Jesse, S.; Tselev, A.; Collins, L.; Yu, P.; Kravchenko, I.; Kalinin, S. V.; Balke, N. "Probing Local Bias-Induced Transitions Using Photothermal Excitation Contact Resonance Atomic Force Microscopy and Voltage Spectroscopy" *ACS Nano* **2015**, *9*, 1848.

[13] Parlak, Z.; Tu, Q.; Zauscher, S. "Liquid contact resonance AFM: analytical models, experiments, and limitations" *Nanotechnology* **2014**, *25*, 445703.

[14] Tung, R. C.; Killgore, J. P.; Hurley, D. C. "Hydrodynamic corrections to contact resonance atomic force microscopy measurements of viscoelastic loss tangent" *Review of Scientific Instruments* **2013**, *84*, 073703.

[15] Tung, R. C.; Killgore, J. P.; Hurley, D. C. "Liquid contact resonance atomic force microscopy via experimental reconstruction of the hydrodynamic function" *Journal of Applied Physics* **2014**, *115*, 224904.

[16] Certain commercial materials and supplies are identified in this paper to foster understanding. Such identification does not imply recommendation or endorsement by the National Institute of Standards and Technology, nor does it imply that the materials or equipment identified are necessarily the best available for the purpose.

[17] Wagner, R.; Raman, A.; Proksch, R. "Spatial spectrograms of vibrating atomic force microscopy cantilevers coupled to sample surfaces" *Applied Physics Letters* **2013**, *103*, 263102.

[18] Killgore, J.; Yablon, D.; Tsou, A.; Gannepalli, A.; Yuya, P.; Turner, J.; Proksch, R.; Hurley, D. "Viscoelastic property mapping with contact resonance force microscopy" *Langmuir* **2011**, *27*, 13983.